NeuroImage 226 (2021) 117558

Contents lists available at ScienceDirect

NeuroImage

journal homepage: www.elsevier.com/locate/neuroimage

Theta rhythm supports hippocampus-dependent integrative encoding in schematic/semantic memory networks

Berta Nicolás[a,b,c], Jacint Sala-Padró[d], David Cucurell[a,b], Mila Santurino[d], Mercè Falip[d], Lluís Fuentemilla[a,b,c,*]

[a] Cognition and Brain Plasticity Group, Bellvitge Institute for Biomedical Research, Hospitalet de Llobregat 08907, Spain
[b] Department of Cognition, Development and Educational Psychology, University of Barcelona, Barcelona 08035, Spain
[c] Institute of Neurosciences, University of Barcelona, Barcelona 08035, Spain
[d] Epilepsy Unit, University Hospital of Bellvitge, 08907 L'Hospitalet de Llobregat, Spain

ARTICLE INFO

Keywords:
Theta rhythm
Hippocampus
Integrative encoding
Episodic memory
Inferential learning

ABSTRACT

Integrating new information into existing schematic/semantic structures of knowledge is the basis of learning in our everyday life as it enables structured representation of information and goal-directed behaviour in an ever-changing environment. However, how schematic/semantic mnemonic structures aid the integration of novel elements remains poorly understood. Here, we showed that the ability to integrate novel picture information into learned structures of picture associations that overlapped by the same picture scene (i.e., simple network) or by a conceptually related picture scene (i.e., schematic/semantic network) is hippocampus-dependent, as patients with lesions at the medial temporal lobe (including the hippocampus) were impaired in inferring novel relations between pictures within these memory networks. We also found more persistent and widespread scalp EEG theta oscillations (3–5 Hz) while participants integrated novel pictures into schematic/semantic memory networks than into simple networks. On the other hand, greater neural similarity was observed between EEG patterns elicited by novel and related events within simple networks than between novel and related events within schematic/semantic memory networks. These findings have important implications for our understanding of the neural mechanisms that support the development and organization of structures of knowledge.

1. Introduction

Experiences often overlap in content, presenting opportunities to integrate them into mnemonic networks. These mnemonic networks share certain characteristics, such as plasticity and hierarchical or schematic/semantic organisation (Eichenbaum 2017), which enable structured representation of information and goal-directed behaviour in an ever-changing environment (McKenzie et al. 2014). However, it remains unclear how such schematic/semantic mnemonic structures aid the integration of new information.

The standard approach to examining integrative encoding into memory networks has been to train subjects on separate episodic events that share common elements (e.g., AB and BC) and then test for the associative network (ABC) via assessment of knowledge about the indirectly associated network elements (AC). This research has shown that the hippocampus and the prefrontal cortex (PFC) are less essential in learning individual associations (AB and BC) than in integrating information across related associated events (AC) (Dusek and Eichenbaum 1997; Greene et al. 2006; Heckers et al. 2004; Preston et al. 2004; Schlichting and Preston 2016). Leveraging the fine-scale temporal resolution of magnetoencephalography (MEG) and electroencephalography (EEG), recent studies have also shown that the integration of novel events into an existing associative memory network relies on hippocampus-driven oscillatory activity in the theta range (3–8 Hz) (Backus et al. 2016; Sans-Dublanc et al. 2017). Thus, while this approach has provided valuable insights into the neural underpinnings supporting the formation of associative memory networks, we still lack understanding of whether a similar neural framework can be generalized to more complex scenarios, akin to real-life environments, whereby several episodes linked by schematic or semantic structures of knowledge foster the assimilation of new events (Van Kesteren et al. 2010, 2012; Packard et al. 2017; Tse et al. 2011).

To address this issue, we designed a two-phase learning and a generalization task (Fig. 1A), wherein participants first learned an intermixed set of picture associations and then learned another set of picture associations that overlapped with the first set, presenting opportunities for generalizing across them. Participants' memory for direct associations and generalization was tested next. We posited two levels of generalized

* Corresponding author.
E-mail address: llfuentemilla@ub.edu (L. Fuentemilla).

https://doi.org/10.1016/j.neuroimage.2020.117558
Received 11 June 2020; Received in revised form 6 November 2020; Accepted 8 November 2020
Available online 25 November 2020

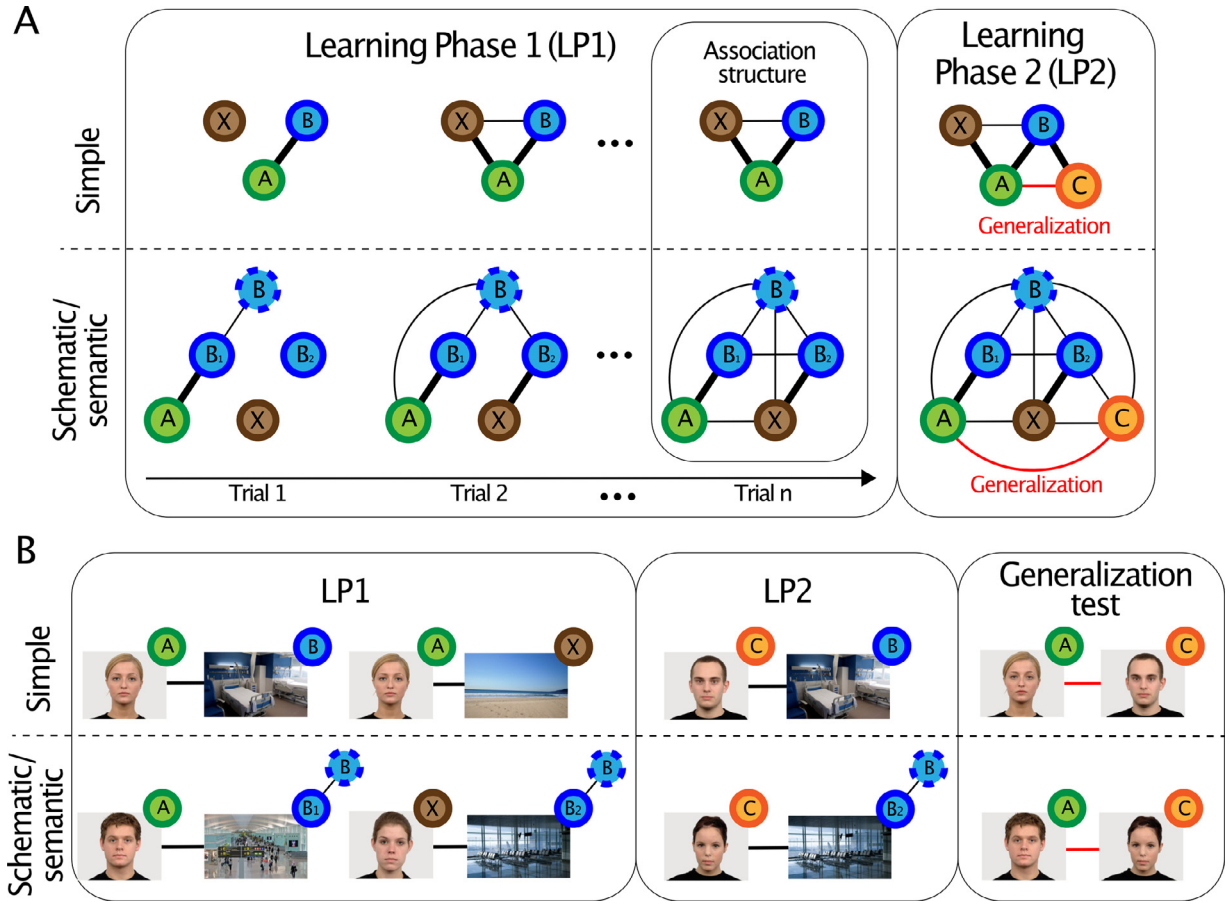

Fig. 1. Memory network models and experimental design. (A) Hypothesized memory representation model accounting for each of the learned picture sets in the simple (A-B and A-X) and schematic/semantic (A-B_1 and X-B_2) conditions throughout LP1. Thick lines depict connections of picture pairs established during learning. Thin lines depict connections of picture pairs established during learning via integrative encoding. At the end of LP1, we hypothesized, several corresponding memory networks were acquired, and their structure reflected a simple condition, wherein new associations were drawn between elements from associations that were already present in memory, or a schematic/semantic typology, wherein new associations were drawn between elements from associations that were already present in memory, but demanded an additional level of association. In LP2, a novel element, C, in the established memory networks from LP1 promoted the binding of a connected set of nodes within each network. (B) In LP1, participants encoded pairs of face-scene images. Picture pairs were organized so that some of them shared the face image (simple condition) and some shared the scene schematic/semantic context (schematic/semantic condition). Picture pair conditions were presented intermixed during LP1. In a following LP2, participants had to learn novel face-scene pairs. All pairs included novel face and scene images that overlapped with one of the scene images from each subset in LP1. Picture pair conditions were presented intermixed during LP2. We tested participants' memory on direct associations (not displayed in the figure) and generalization.

associations: "simple", wherein new associations were drawn between elements from associations that were already present in memory (on which subjects had already been trained); and "schematic/semantic", wherein new associations were drawn between elements from associations that were already present in memory, but demanded an additional level of association (i.e., a semantic or schematic relationship between elements that is assumed to be pre-existing or "common knowledge").

During learning phase 1 (LP1), participants learned to associate a face with a scene by choosing which of two scenes went with the face, and then receiving feedback. While each face-scene association was learned individually, there was partial overlap across events. Some pairs overlapped with a common face picture (A-B and A-X; simple network condition) and other pairs with scene pictures from the same semantic category (A-B_1 and X-B_2; schematic/semantic network condition) (Fig. 1B). By the end of LP1, we expected that participants would have successfully learned the individual associations and integrated them based on their relational network properties, namely simple or schematic/semantic (Fig. 1B).

To assess whether these two mnemonic network structures influenced integrative encoding of new information, we next asked participants to encode a novel set of face-scene picture associations (i.e., learning phase 2, LP2), wherein each scene picture corresponded to a scene from the mnemonic picture set learned in LP1 (Fig. 1B). Thus, we expected that the overlap between scene images (B and B_1 in Fig. 1B) would induce the integration of the new face images (i.e., C) into the specific memory network learned in LP1, thereby promoting generalization (Fig. 1B). Thus, in LP2, trials from the two conditions were similar in their configuration (face – scene) and in the content of the picture that overlapped with picture sets from LP1 (i.e., scenes), thereby allowing to infer that any possible difference in the elicited neural patterns could be attributed to the integrative encoding mechanisms linked to the memory network properties established in LP1.

After LP2, participants were tested using a two-alternative forced choice paradigm that included directly learned association trials ("trained") as well as inference trials that tested participants' ability to generalize. Specifically, "generalization" trials tested whether participants would choose A, encoded in LP1, when presented C, encoded in LP2 (Fig. 1B), thereby assessing whether they had successfully integrated LP2 events into the related memory structures acquired in LP1.

Here, we first aimed at examining whether events encoded in LP2 elicited similar or different theta oscillatory patterns as a function of whether they were linked to simple or schematic/semantic memory net-

Table 1
Individual patient characteristics.

Diagnosis	Gender	Age	IQ	Years Educ.	Years since onset	Clinical notes /aetiology	Treatment
R-MTL	M	53	100	20	12	Arterio-venous malformation	Carbamazepine 600 mg/day Brivaracetam 150 mg/day
R-MTL	F	52	80	12	15	Cavernoma	Lacosamide 250 mg/day
L-MTL	M	26	80	8	12	Encephalocele	Escicarbazepine 160 mg/day Perampanel 8 mg/day Clobazam 20 mg/day
R-MTL	F	46	90	8	9	PET hypometabolism	Lacosamide 200 mg/day Levetiracetam 3000 mg/day Eslicarbazepine 1200 mg/day
R-MTL	F	38	137.5	17	6	Amygdalar dysplasia	Duloxetine 90 mg/day Eslicarbazepine 800 mg/day Levetiracetam 500 mg/day Lacosamide 150 mg/day Clobazam 10 mg/day
L-MTL	M	43	95	12	30	Parieto-temporal gliosis	Eslicarbazepine 400 mg/day Pregabaline 225 mg/day
L-MTL	F	70	80	8	28	PET hypometabolism	Carbamazepine 400 mg/day Clobazam 15 mg/day
R-MTL	M	56	110	13	43	Hippocampal sclerosis	Topiramate 100 mg/day Eslicarbazepine 1600 mg/day Levetiracetam 200 mg/day Perampanel 8 mg/day
L-MTL	M	35	90	21	5	PET hypometabolism	Eslicarbazepine 1600 mg/day Zonisamide 500 mg/day Perampanel 2 mg/day
L-MTL	F	57	100	12	13	Hippocampal sclerosis	Escitalopram 10 mg/day Lamotrigine 400 mg/day Clobazam 5 mg/day
R-MTL	F	26	110	21	3	PET hypometabolism	Perampanel 4 mg/day Levetiracetam 300 mg/day
L-MTL	M	51	90	8	29	Hippocampal sclerosis	Phenobarbital 100 mg/day Levetiracetam 3000 mg/day Eslicarbazepine 1600 mg/day
R-MTL	M	57	80	7	49	Hippocampal sclerosis	Carbamazepine 600 mg/day Levetiracetam 4000 mg/day Zonisamide 300 mg/day
R-MTL	M	53	95	20	13	Arterio-venous malformation	Carbamazepine 600 mg/day Brivaracetam 150 mg/day

works acquired in LP1. Second, prior literature has emphasized that inferential learning relies on the reactivation of memory events related to a network (e.g., Zeithamova et al., 2012). In the current study, we implemented a time-resolved neural similarity analysis (e.g., Silva et al., 2019; Sols et al. 2017) to elucidate whether LP2 events elicited the reactivation of elements within a schematic/semantic and simple memory network. And third, we examined the critical role of the hippocampus in integrative encoding for simple and schematic/semantic memory networks by comparing behavioural data from chronic epileptic patients with hippocampal lesions with data from a matched control sample.

2. Material and methods

2.1. Participants

Experiment 1: Healthy adults. Forty right-handed healthy volunteers (34 women) participated in the experiment 1. Mean age of the participants was 23.62 (SD = 2.98 years). All the participants included in the study reported no history of medical, neurological, or psychiatric disorders, and no drug consumption. All subjects were volunteers, gave written informed consent, consented to publication, and received financial compensation for their participation in this study. All participants had normal or corrected-to-normal vision. The study was approved by the Ethics Committee of the University of Barcelona.

Experiment 2: TLE patients. A group of fourteen patients (6 women; mean age = 47.36 years old (SD = 12.54); mean years of education was 13.36 (SD = 5.40)) with refractory mesial temporal lobe epilepsy (TLE) caused by different aetiologies was recruited following a pre-surgical evaluation at the University Hospital of Bellvitge (Table 1). All patients had sustained damage to the right or left anterior medial temporal lobe structures, including the hippocampus. In all patients, verbal and non-verbal intelligence was assessed using the Weschler Memory Scale, and the mean IQ was 95.54 (SD = 15.9). Patient diagnosis was established according to clinical, EEG, and magnetic resonance imaging or FDG18PET. All of the patients underwent neurological and neuropsychological examination, continuous video-EEG monitoring, and structural and functional neuroimaging (MRI and PET). Patients were included in the study when the clinical data, EEG findings, and neuroimaging data suggested unilateral mesial TLE. All patients had: 1) seizures with typical temporal lobe semiology that were not controlled with antiepileptic drugs, 2) EEG patterns concordant with mesial temporal lobe epilepsy, and 3) neuroimaging data supportive of hippocampal involvement in seizure generation. None of the patients suffered a seizure during the experimental task or 24 h before the task, and all of the patients were on habitual anti-epileptic drug regimens. The study was approved by the Ethical Committee of University Hospital of Bellvitge. Informed consent was obtained from all of the patients before participation in the study.

Experiment 2: Healthy controls. The control group consisted of fourteen participants with no history of neurological disorders. Control participants were individually matched to TLE patients. Mean age of the control group was 46.64 years old (SD = 12.42) and mean years of education was 13.71 (SD = 5.41). No differences were found between groups in terms of age (t (26) = 0.15, $p = 0.89$) or years of education (t (26) = -0.17, $p = 0.86$). Informed consent was obtained from all subjects before their participation in the study.

2.2. Experimental procedures

Stimuli. Stimuli consisted of 24 images of Caucasian (half women) non-expressive faces (F) from Radboud database (Langner et al. 2010) and from UT Dallas database (Minear and Park 2004) and 48 scene (S) images selected to depict 48 real-life contexts, half of them from indoor context scenes (bars, airports, hospitals, supermarkets, kitchens, bakeries, hairdresser's, clothing stores, locker room, cinema, bus stop, ice-cream shop, computer store, campsite, jail) and the other half from outdoor context scenes (parks, landscapes, waterfalls, mountains, caves, beaches, lakes, forests), from SUN database (Xiao et al. 2010).

The faces were distributed through LP1 (8 for the simple and 16 for the schematic/semantic experimental condition), LP2 (8 for each experimental condition), generalization (8 for each experimental condition), and trained test (16 each experimental condition). Scene context images were distributed over LP1 (16 for each experimental condition) and were repeated over LP2 (8 for each experimental condition) and trained test (16 for each experimental condition). F-S pair assignments were randomized between participants. The order of F-S picture presentation was randomized within each LP1 and LP2 block.

Task design and procedure in healthy participants (Experiment 1). Participants performed a modified version of an associative inference task (e.g., Zeithamova et al., 2012) (Fig. 1). The task consisted of two separate learning phases, Learning Phase 1 (LP1) and Learning Phase 2 (LP2), followed by a Testing Phase. In each of the learning phases, participants were requested to learn Face (F) – Scene (S) associations through feed-

back. Unbeknownst to the participants, in LP1 F-S associations were organized into eight picture subsets, each including two F-S pairs. Subsets in the simple condition involved one face image (e.g., F1) which was associated with two different scene images (e.g., S1 and S2). During LP1, F1 was presented separately with S1 and S2 in separate trials, thereby promoting inferential learning between S1 and S2 through associative overlap. Picture subsets in the schematic/semantic condition involved two different face images (e.g., F2 and F3) and two different scene images (e.g., S3 and S4) from the same semantic category. During LP1, F2-S3 and F3-S4 pair associations were presented in separate trials. Specific F-S pairs in the simple and in the schematic/semantic condition were randomly assigned before the experiment started. LP1 was structured into 8 blocks separated by brief pauses to the participants. Each block included 32 trials in total (16 trials per experimental condition). LP1 was followed by LP2, which consisted of 16 different F-S pairs presented 8 times throughout the 8 blocks. Importantly, in LP2 all face images were novel but each of them was paired with a scene image from a subset of picture scenes presented in LP1. Thus, in LP2 8 faces were associated with 8 scenes from the simple condition subsets from LP1 (henceforth, simple condition) and 8 faces were presented with 8 scenes from each of the schematic/semantic condition subsets from LP1 (schematic/semantic condition), thereby providing opportunities for integrative encoding of picture subsets from LP1 that had differential relational structure (i.e., simple or schematic/semantic).

The structure of the trials was similar in LP1 and LP2. Each trial consisted of the presentation of a face at the top of the screen and two scenes at the bottom for 3500 ms. Participants had to wait for the appearance of the message 'RESPONSE' and they then had 1000 ms to indicate, by pressing a button, which of the two scenes was associated with the face. Following participants' choices, a delay period (grey background) of 500 ms preceded the feedback, which consisted of the presentation of a green tick (right choice) or a red X (wrong choice), each of which remained on the centre of the screen for 1000 ms. The appearance of the correct scenes on the right or left side of the screen was counterbalanced through the presentations. Additionally, in order to avoid stimulus-response learning strategies, every scene was shown as a correct choice for a particular face and as an incorrect choice when appearing with other faces, with the restriction that it could not appear twice as an incorrect choice with the same face. Therefore, the correct scene for a given face was always the same, but the incorrect scene was variable.

Two separate surprise force-choice tests followed LP2: the generalization and the trained test. In the generalization test, participants had to indicate which of two faces seen during LP1 was associated with a face from LP2 presented at the top of the screen, thereby assessing inferential learning. This test consisted of 16 trials (8 for each experimental condition). In the trained test, two scene images appeared, and participants had to indicate which had been associated with the face image presented at the top of the screen. This test always followed the generalization test, thereby ruling out the possibility that accuracy in the inferential test could be explained by other factors (i.e., memory recall for pair associates) other than neural mechanisms elicited during LP2. In this test, all trained pairs from LP1 and LP2 were tested. In the generalization and direct test, the incorrect choice elements were all previously learned items that had been studied during the task. Pictures remained on screen until the participants responded, and there was no feedback informing the participants of the result of their choice. Test trials were separated by an inter-trial time randomized between 750 and 1250 ms.

Task design and procedure in TLE patients and healthy controls (Experiment 2). A shorter version of the experiment 1 task was implemented in TLE patients and control samples. More concretely, LP1 consisted of 12 subsets of F-S associations: 6 from the simple condition and 6 from the schematic/semantic condition. All pairs were presented 8 times throughout 8 different blocks. LP2 consisted of 6 face-scene associations (3 from the simple condition and 3 from the schematic/semantic condition). At the end of the task, a generalization test consisting of 6 possible face-face associations, and a trained test consisting of 12 possible face-scene associations were implemented.

Behavioural analysis. Participants' correct responses throughout LP1 and LP2 were calculated and averaged for each block of trials. A repeated measures ANOVA including Block (8 levels) and experimental condition (simple and schematic/semantic) as within-subject factors was used for statistical assessment. Participants' accuracy in the tests was assessed by the proportion of correct choices separately for the generalization test and the trained test. Statistical significance was set at an alpha of 0.05. Greenhouse-Geisser epsilon correction was used to correct for possible violations of the sphericity assumption for statistical analysis when necessary; the adjusted p-values after the correction were reported.

EEG recordings and preprocessing in Experiment 1. EEG was recorded at a 500 Hz sampling rate (High-pass filter 0.01 Hz, notch filter at 50 Hz) from the scalp using a BrainAmp amplifier and tin electrodes mounted on an electrocap (Electro-Cap International) located at 29 standard positions (Fp1/2, Fz, F7/8, F3/4, FCz, FC1/2, FC5/6, Cz, C3/4, T3/4, Cp1/2, Cp5/6, Pz, P3/4, T5/6, PO1/2, Oz) and at the left and right mastoids. An electrode placed at the lateral outer canthus of the right eye served as an online reference. EEG was re-referenced offline to the linked mastoids. Vertical eye movements were monitored with an electrode at the infraorbital ridge of the right eye (EOG channel). Electrode impedances were kept below 3 kΩ. EEG was band-pass filtered offline at 0.1–40 Hz. Independent Component Analysis was applied to the continuous EEG data to remove blinks and eye movement artefacts. Trials exceeding $\pm$ 100 μV in both EEG and EOG within a -100 to 2500 ms time window from stimulus onset were rejected offline and not used in the time-frequency and neural similarity analysis detailed below. 7 participants were excluded from subsequent EEG analyses as they did not produce at least 5 artefact-free trials for each of the 8 learning blocks in LP2.

Time-frequency (TF) analysis. TF was performed using six-cycle complex Morlet wavelets in 7100 ms EEG epochs (2100 ms before stimulus onset through 5000 ms after) from LP2. Changes in time-varying energy (square of the convolution between wavelet and signal) in the 1–12 Hz band were computed for each trial and averaged separately for each experimental condition at the individual level. Before performing an overall average, power activity changes were computed with respect to the baseline of each participant (-200 to 0 ms from picture onset).

Similarity analysis. This analysis was set to assess for the possibility that the encoding of LP2 picture pairs elicited the reactivation of neural patterns triggered by picture pairs from the same memory network acquired in LP1, thereby suggesting, according to previous reports investigating inferential learning (Zeithamova et al., 2012), that neural reactivation arises as a mechanism supporting integrative encoding during LP2. To address this issue, we implemented a time-resolved trial-to-trial similarity analysis between EEG patterns elicited during the last block in LP1 and EEG patterns elicited throughout LP2. Only EEG data elicited from LP1 trials that did not share any overlap with LP2 face-scene pairs were used in this analysis. Thus, any difference in similarity patterns between conditions may likely reflect the reinstatement of distinct network association structure that are thought to underly simple and schematic/semantic conditions in the current experiment. Furthermore, we reasoned that including trials only from the last LP1 block guaranteed that neural patterns taken in the analysis were the strongest and most stable memory traces associated with each picture pair in LP1, as learning accuracy in that block was almost perfect and similar between experimental conditions (see results below).

The similarity analysis was performed at the individual level, and included spatial (i.e., scalp voltages from all the 29 electrodes) and temporal features, which were selected in steps of 10 sample points (20 ms) of the resulting z-transformed EEG single-trials. Similarity analysis was implemented at single-trial level by correlating point-to-point the spatial EEG features throughout 2500 ms from picture onset. The similarity analysis was calculated using Pearson correlation coefficients, which are insensitive to the absolute amplitude and variance of the EEG response.

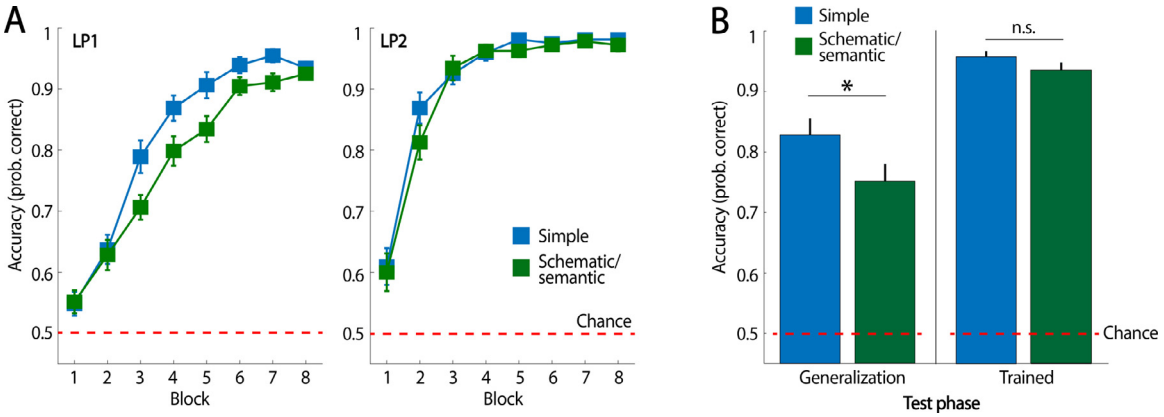

Fig. 2. Behavioural data in healthy young participants (Experiment 1). (A) Averaged participants' accuracy in selecting the correct scene association with a given face throughout LP1 and LP2 for each experimental condition. (B) Averaged participants' accuracy in the generalization and the trained memory tests. $^{*}p < 0.05$ and n.s., $p > 0.05$. Error bars indicate standard error of the mean.

R values were then Fischer z scored before statistical comparison analysis.

Cluster statistics of the EEG data. To assess for power differences between conditions at the temporal domain, we used a paired sample permutation test (Groppe, Urbach, and Kutas 2011) to deal with the multiple comparisons problem given the multiple sample points included in the analysis. This test uses the "*t* max" method to adjust the p-values of each variable for multiple comparisons (Blair and Karniski, 1993). Like Bonferroni correction, this method adjusts p-values in a way that controls for the family-wise error rate.

To account for scalp distribution differences (i.e., spatial dimension) between simple and schematic/semantic conditions in time-frequency data and to account for differences between conditions in the similarity analysis (i.e., temporal dimension), a cluster-based permutation test was used (Maris and Oostenveld 2007), which identifies clusters of significant points in the resulting 2D matrix in a data-driven manner and addresses the multiple-comparison problem by employing a nonparametric statistical method based on cluster-level randomization testing to control for the family-wise error rate. Statistics were computed for each time point, and the time points whose statistical values were larger than a threshold ($p < 0.05$, two-tail) were selected and clustered into connected sets on the basis of x, y adjacency in the 2D matrix (defined by at least 2 contiguous points). The observed cluster-level statistics were calculated by taking the sum of the statistical values within a cluster. Then, condition labels were permuted 1000 times to simulate the null hypothesis, and the maximum cluster statistic was chosen to construct a distribution of the cluster-level statistics under the null hypothesis. The nonparametric statistical test was obtained by calculating the proportion of randomized test statistics that exceeded the observed cluster level statistics.

3. Results

3.1. Experiment 1 (Healthy participants)

Behavioural performance. All participants were able to learn face-scene associations from the simple and schematic/semantic condition in LP1 (Fig. 2A). This was reflected by high accuracy (i.e., > 90%) in the participants' ability to choose the association pair correctly in the two conditions in the last block of the encoding (paired t-test: t (39) = 1.50; $p = 0.14$). A repeated-measures ANOVA including condition (simple and schematic/semantic) and block (from one to eight) as within-subject factors confirmed accuracy improvement over the course of the task for all subsets of pictures (main effect of block: F (4.03,157.22) = 174.96, $p < 0.01$). However, that increment was less steep in the schematic than in the simple condition (Condition x block effect: F (5.01,195.47) = 2.51, $p = 0.016$).

In LP2, participants reached high levels of accuracy relatively rapidly and they were highly accurate (i.e., > 90%) in selecting the correct association by the end of the learning phase (Fig. 2A). A repeated-measures ANOVA, including experimental condition and block as within-subject factors, revealed no significant differences between conditions (F (1,39) = 2.56, $p = 0.12$) or experimental condition x block (F (7,273) = 0.78, $p = 0.60$). A trend towards significance was found for the block factor (F (5.20,202.99) = 1.87, $p = 0.07$), indicating that participants' learning occurred very rapidly during encoding and reached a ceiling effect at early stages of the encoding rounds.

Participants showed, overall, high accuracy in the generalization test, thereby demonstrating that they had successfully integrated picture sets from LP1 during LP2 (Fig. 2B). However, we found that accuracy was greater in the simple (Mean = 82.81%, SD = 17.15%) than the semantic/schematic condition (Mean = 75%, SD = 18.95%) (t (39) = 2.48, $p = 0.018$). Importantly, participants were highly accurate in the trained test (i.e., > 80%) and their performance did not differ between conditions (t (39) = 1.36, $p = 0.18$) (Fig. 2B), thereby confirming that they retained the trained associations from the two experimental conditions in equal measure. Altogether, the behavioural findings suggest that the underlying structure of the associations learned during LP1 may have had an impact during encoding strategies in LP2, which is when participants had the possibility to create the relational links needed to establish inferential learning between face-scene pairs.

Theta oscillations. To determine which frequency ranges showed a modulation in response to stimuli from the two experimental conditions in in LP2 we compared frequency-to-frequency power values from the baseline period (averaged over all sensors and -200 to 0 ms from picture onset) and post-stimuli onset (1 to 2500 ms from picture onset). The results of this analysis are depicted in Fig. 3A and the stimuli input elicited significant ($p < 0.05$, uncorrected) changes at 3–5 Hz, within the theta band, and at 8–12 Hz, within the alpha band. Next, we sought to examine whether power modulations at these frequency ranges differed during LP2 as a function of whether stimuli input belonged to the simple or the semantic/schematic condition. This analysis revealed that theta, but not alpha, power increase was more extended in time in response to picture pairs that were linked to semantic/schematic, as compared to simple memory structures acquired in LP1 (Fig. 3B and C). A cluster-based permutation test revealed that the persistent theta power increase in the schematic condition as compared to the simple condition was distributed over the scalp, spanning frontal, central, and posterior scalp sensors (Fig. 3C).

Having found enhanced theta power in response to stimuli associated with schematic/semantic memory networks during LP2, we

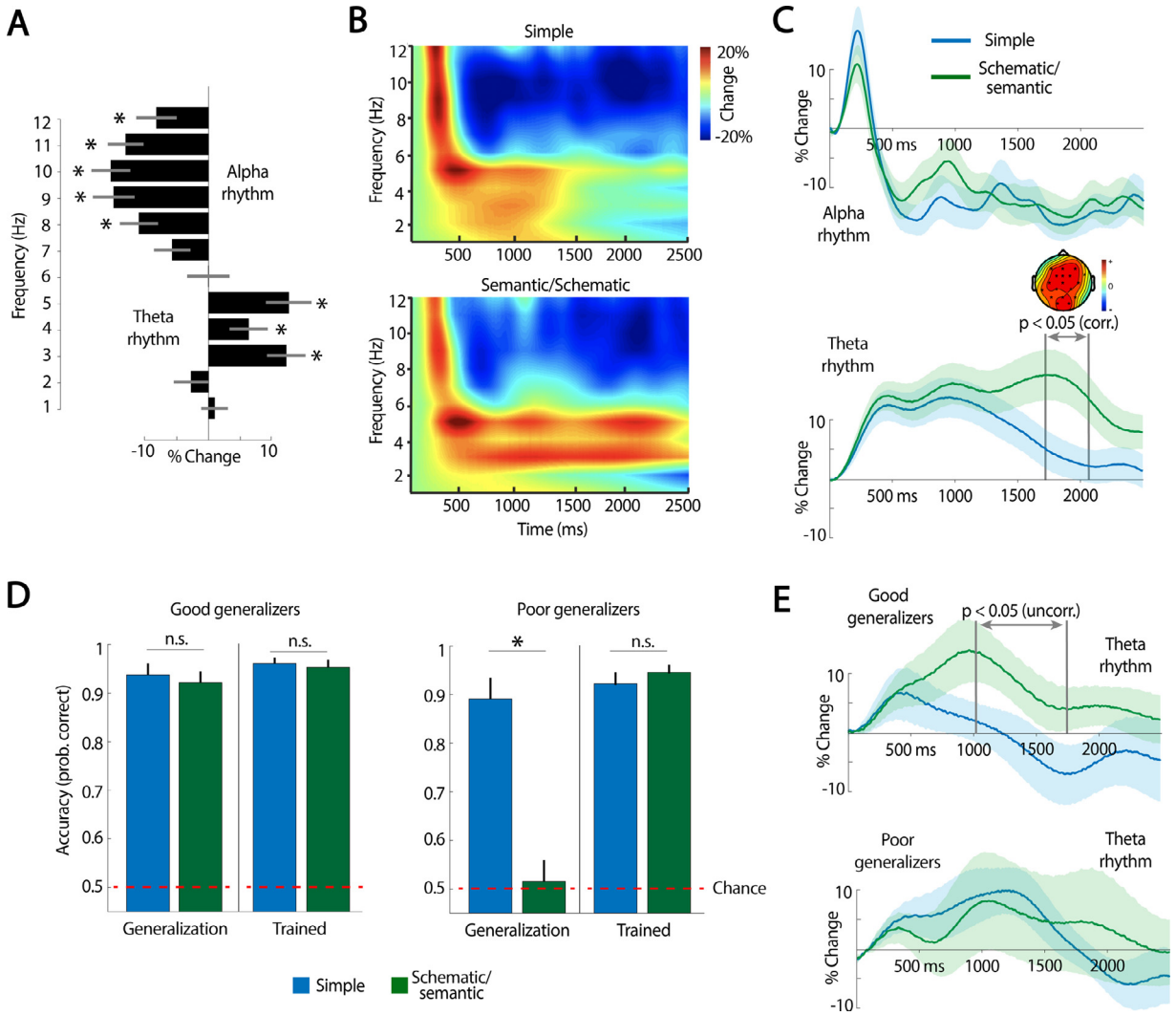

Fig. 3. Theta oscillations in LP2. (A) Group-averaged changes in spectral power with respect to the baseline (-200 to 0 ms from picture onset), averaged over all scalp sensors and temporal window from stimuli onset (1 to 2500 ms) averaged over the two experimental conditions in LP2. Statistically significant increases in power within the theta range and power decrease in frequencies within the alpha range are marked with an asterisk ($p < 0.05$, two-tailed, uncorrected). (B) Group-averaged changes in spectral power with respect to the baseline (-200 to 0 ms from picture onset) (averaged over all scalp sensors) elicited by picture pairs from the simple and semantic/schematic conditions in LP2. (C) Changes in theta (averaged of 3–5 Hz) and alpha (averaged of 8–12 Hz) power relative to pre-stimuli baseline for the two experimental conditions in LP2. A power increase in the alpha and theta band was observed in both conditions. However, statistical differences between conditions were only observed at the theta band. Significant time points corrected for multiple comparison were between 1772 and 2024 ms after stimuli onset ($p < 0.05$; one-tail). Spatially distributed theta differences between simple and schematic/semantic conditions are also depicted; sensors that were significant and corrected for multiple comparisons at cluster level are marked with a black asterisk. (D) We split the participants into two groups. Participants were selected according to the first and last quartile of the sample based on their generalization performance in the schematic/semantic final test. $^{*}p < 0.05$ and n.s., $p > 0.05$. Error bars indicate standard error of the mean. (E) Changes in theta power (averaged of 3–5 Hz and scalp EEG sensors) in Good and Poor generalizers relative to pre-stimuli baseline for the two experimental conditions in LP2. Significant time points were between 1010 and 1740 ms after stimuli onset ($p < 0.05$, one-tail, uncorrected). Thick lines represent in (C) and (D) the mean across participants and point-to-point standard error is depicted in shaded colour.

asked whether this effect was seen in participants that performed well in the generalization tests but not in those participants who failed to be accurate specifically in the generalization test for the schematic/semantic condition. To test this issue, we split the participants into 2 groups. We selected the first and last quartile of the sample based on the accuracy in the generalization test. Importantly, as the aim of this testing was to look for an effect associated solely with the generalization on the schematic/semantic condition, we formed the subgroups with the restriction that, between them, they were similar in their accuracy for trained associations and in their generalization accuracy in the simple condition but not in the schematic/semantic condition. This yielded "Good" (n = 8) and "Poor" (n = 8) generalizers (Fig. 3D), who, despite being similar in their memory accuracy for trained associations (Simple condition: Good, 96.1% ± 3% and Poor, 92.19% ± 7%; schematic/semantic condition: Good, 95.31% ± 4% and poor, 94.53% ± 5%; condition x group, $F(1,14) = 0.57$, $p = 0.46$), markedly differed in their ability to generalize on the schematic/semantic condition (Simple condition: Good, 93.75% ± 7% and Poor, 89.1% ± 12%; schematic/semantic condition: Good, 92.19% ± 11% and Poor, 51.56% ± 12%; condition x group, $F(1,14) = 42.56$, $p < 0.01$). Post-hoc 2 sample t-test confirmed that the 2 groups differed only in schematic/semantic ($t(14) = 8.22$, $p < 0.01$) but not in the simple ($t(14) = 0.94$, $p = 0.36$) condition at the generalization test.

Having homogenized participants' subsamples by their ability in trained pairs and in generalizing in the simple condition only, we

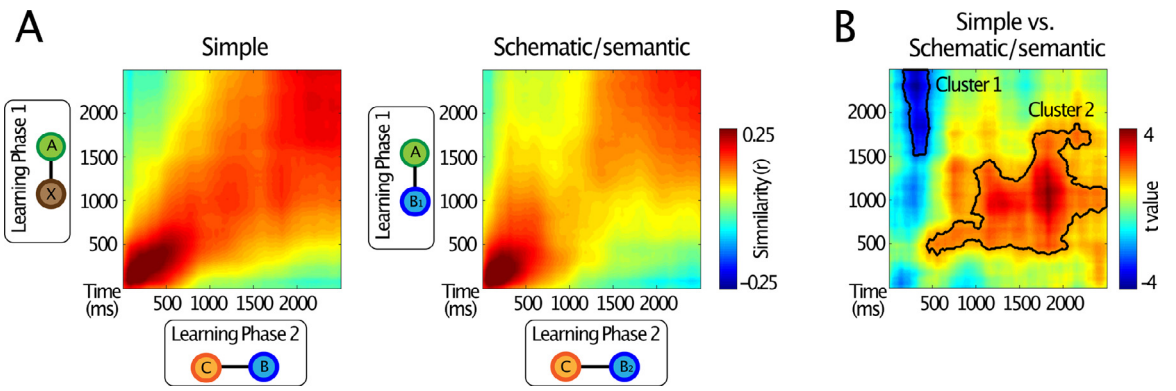

Fig. 4. Neural pattern similarity between events that overlapped within memory network structures in the task. (A) Group-averaged time-resolved degree of similarity between A-X/A-B_1 events from the last block of trials in LP1 and the corresponding A-B and C-B_2 trials during LP2. Neural similarity in this analysis offers a measure of how similar two neural patterns are when elicited by events which, although separated in time, share partial memory information in the current task. Here, the partial memory information is not explicit recall because the trials compared did not include any overlapping face or scenes. What is shared is the association structure: in both conditions, this was the A-C link (which was never explicitly presented). (B) Point-to-point *t* value map from comparing schematic/semantic and simple neural similarity results. Two clusters of statistically significant similarity values were found ($p < 0.05$, cluster-based permutation test) (indicated by a thick black line).

next examined whether theta activity differed between them. Indeed, we found higher theta power response to stimuli associated to the schematic/semantic condition with stimuli associated to the simple condition in Good generalizers. This was not the case for Poor generalizers (Fig. 3E).

Neural similarity. This analysis revealed that the patterns of EEG responses elicited by picture pairs in the last LP1 block correlated with EEG patterns elicited during the encoding of different picture pairs that overlapped in content (Fig. 4A). However, the degree of neural similarity differed between experimental conditions. More specifically, picture pairs linked to learned picture pairs in LP1 from the simple condition showed significantly stronger neural similarity values over a window of ~500 to 2000 ms from stimulus onset in LP2. On the other hand, EEG patterns elicited by picture pairs in the schematic/semantic condition showed an increased neural similarity earlier in time during the encoding of linked LP2 picture pairs (at around 300–500 ms from LP2 picture onset) (Fig. 4B). In addition, the same analysis of LP1 trials from the first block during learning did not show any statistically significant differences between trial conditions, thereby suggesting that the similarity effects were greatest when neural patterns reflected robust memory representations of network representations at the end of LP1.

3.2. Experiment 2 (TLE patients and matched controls)

In line with experiment 1, a mixed-design ANOVA, including condition and block as a within-subject factor and group (TLE and control) as a between factor in LP1 data, revealed a statistically significant main effect in condition ($F(1,26) = 5.14$, $p = 0.03$) and block ($F(7,182) = 19.35$, $p < 0.01$), and a non-significant condition x block interaction ($F(7,182) = 1.37$, $p = 0.22$), which indicated that TLE patients and controls successfully encoded picture pairs over the task. No significant differences were found between groups in any of the contrasts (i.e., condition x group: $F(1,26) = 0.6$, $p = 0.81$, block x group: $F(7,182) = 1.66$, $p = 0.12$; and condition x block x group: $F(7,182) = 2.03$, $p = 0.053$). The same statistical analysis of behavioural data from LP2 revealed that both groups successfully acquired picture pairs over the course of the task (block effect: $F(4.13,107.37) = 15.64$, $p < 0.01$; block x group interaction: $F(7,182) = 0.80$, $p = 0.58$), independently of the experimental conditions (condition effect: $F(1,26) = 0.03$, $p = 0.87$; condition x group interaction: $F(1,26) = 1.11$, $p = 0.30$); condition x block x group: $F(7,182) = 0.95$, $p = 0.47$)) (Fig. 5A).

We next assessed for group differences in the generalization and trained test through an ANOVA, including test type (trained and generalization), condition (Simple and Schematic/semantic) as within-subject factors and group (TLE and control) as a between-factor factor. This analysis revealed a statistically significant main effect of group ($F(1,26) = 11.37$, $p < 0.01$) and a group x test type x condition effect ($1,26) = 4.74$, $p = 0.03$) but not any other statistically significant x group interaction effect (test type x group: $F(1,26) = 2.42$, $p = 0.13$; condition x group: $F(1,26) < 0.1$, $p = 0.89$). This indicated the TLE and controls' response accuracy differed as a function of test type and condition. To try to identify the source of this triple interaction, we first searched for group differences in the generalization test through another ANOVA, including condition and group as a within- and between-subject factors, respectively. This analysis revealed a significant main effect of group ($F(1, 26) = 9.22$, $p = 0.005$) but not of condition ($F(1, 26) = 0.59$, $p = 0.45$), nor a condition x group interaction ($F(1, 26) = 1.30$, $p = 0.26$) (Fig. 5B). This indicated that TLE patients showed poorer ability to generalize in the simple and schematic/semantic condition. In fact, while behavioural accuracy in each of the conditions was high and above chance in healthy controls (Simple: $t(13) = 6.87$; $p < 0.01$; Schematic/semantic: $t(13) = 2.57$; $p = 0.02$), TLE patients performed at chance in the tests (Simple: $t(13) = 0.31$; $p = 0.76$; Schematic/semantic: $t(13) = 0.30$; $p = 0.76$). A paired-sample *t*-test analysis showed that accuracy did not differ statistically between conditions at within group level (controls: $t(13) = 1.82$, $p = 0.09$; TLE patients: $t(13) < 0.5$).

We then repeated the same ANOVA strategy regarding memory accuracy for trained events. An ANOVA including condition and group as a within- and between-subject factors, respectively, showed a significant group ($F(1,26) = 13.61$, $p = 0.01$) but not a group x condition interaction effect ($F(1,26) = 2.13$, $p = 0.16$). This indicated that TLE patients were less accurate in recognising the individual face-scene associations acquired during LP2 when compared to controls (Fig. 5B). Importantly, both controls and TLE patients showed consistent above-chance performance in each of the test measures (controls – simple condition: $t(13) = 14.14$; $p < 0.01$; controls – schematic/semantic: $t(13) = 20.21$; $p < 0.01$; TLE patients – simple: $t(13) = 1.94$; $p = 0.07$; TLE patients – schematic/semantic: $t(13) = 5.1$; $p < 0.01$). A paired-sample *t*-test analysis showed that accuracy did not differ statistically between conditions at within-group level (controls: $t(13) = -0.56$, $p = 0.58$; TLE patients: $t(13) = -1.33$, $p = 0.21$).

4. Discussion

A challenge in memory research has been to understand how structures of knowledge can aid integrative encoding of new information. Here, we showed that process may be mediated by hippocampus activ-

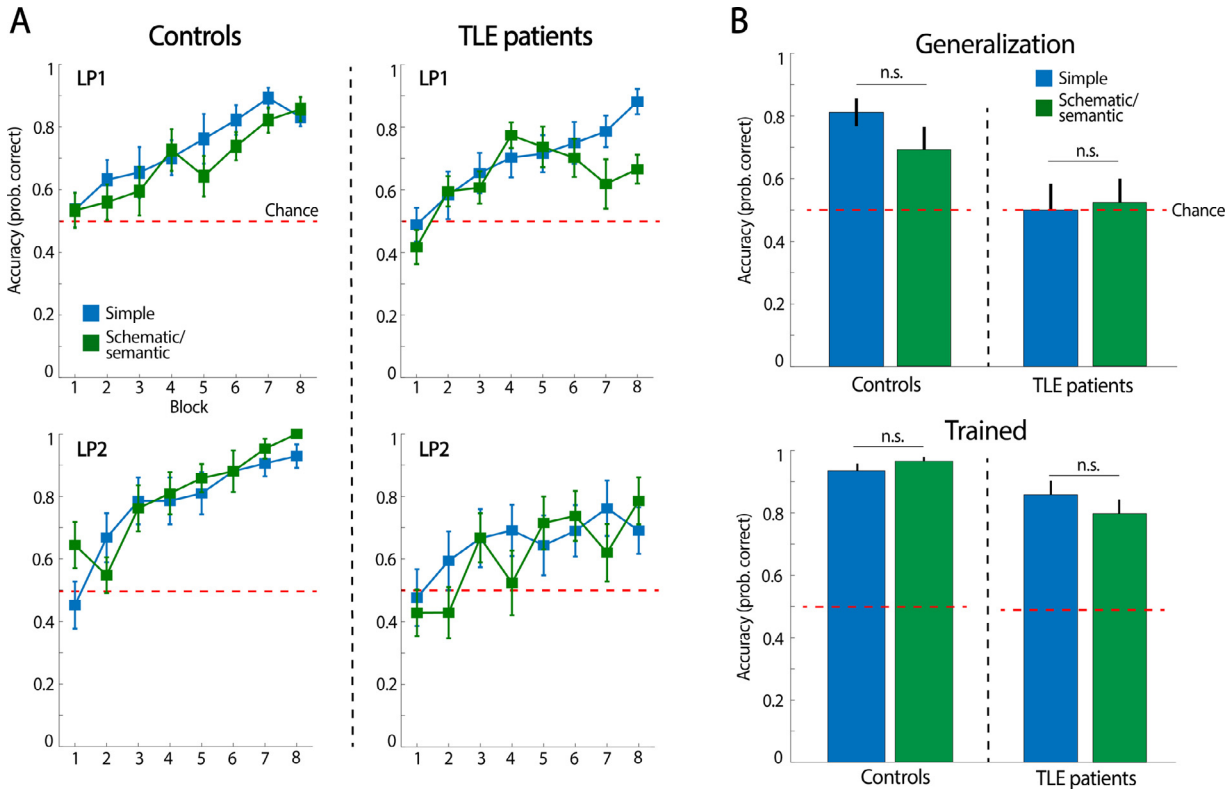

Fig. 5. Behavioural data in TLE and healthy control participants (Experiment 2). (A) Averaged participants' accuracy in selecting the correct scene association with a given face throughout LP1 and LP2 for each experimental condition. (B) Averaged participants' accuracy in the generalization and trained memory tests. $^{*}p < 0.05$ and n.s., $p > 0.05$. Error bars indicate standard error of the mean.

ity, as TLE patients were impaired in inferring novel relations between elements within mnemonic networks. In addition, we observed more persistent and widespread theta activity (3–5 Hz) in the scalp during the encoding of novel pictures integrated into existing schematic memory networks, emphasizing the role that theta oscillations may play in inferential learning. Finally, we found higher similarity values for neural activity patterns elicited by novel and related events within simple networks, thereby suggesting that neural reactivation may be important in integrative encoding when novel information relates to a mnemonic network of elements linked by direct associations.

Our findings provide evidence that MTL structures, including the hippocampus, are essential to enabling the rapid integration of new information within stored knowledge in a schematic structure. These results align well with previous studies that revealed the critical role of the hippocampus in inferential learning between different episodic events that overlap in the perceptual content in healthy individuals (Schlichting and Preston 2015; Zeithamova et al., 2012) and in patients with lesions in the MTL (Pajkert et al. 2017). However, the current results extend these findings by showing that the disruption of lower-level inferential learning (i.e., simple generalized associations in our study) may also prevent the kind of higher-level learning tested herein under schematic/semantic generalized associations. In fact, the notion that the hippocampus is critical in encoding new experiences into congruent schematic memories has received support from animal (Tse et al., 2011) and human studies (Van Kesteren et al. 2010b; Schlichting and Preston 2015). Interestingly, the degree to which hippocampal integration mechanisms identified in episodic inference contribute to other forms of generalization, such as concept learning, has often been neglected in the literature. For example, recent fMRI findings in humans showed that the anterior hippocampus, in concert with the PFC, generated and tracked the prototype representation of multiple items that overlapped in their content during a learning phase. The degree to which participants in that study relied on such conceptual representation abstracted across the training set predicted their ability to generalize into novel items in a later test. (Bowman and Zeithamova 2018).

The notion that prior knowledge, and schema representations in particular, has an impact in memory has been long observed in psychological research (e.g., Bartlett, 1932; Craik and Lockhart 1972). However, the investigation of how schemas influence memory formation has suffered from the heterogeneous usage of the term in neuroscience. In the current study, we labelled schematic/semantic memory to a set of complex interrelated picture associations in a network that incorporates many of the necessary features that are thought to qualitatively differ from a purely (i.e., simple) associative memory network (Ghosh and Gilboa 2014). Indeed, here schematic/semantic memory networks are defined by an associative network structure that is organized in a hierarchal fashion. It emerges based on multiple episodic exposure to representational units that lack a unit of detail (i.e., their elements are interrelated via semantic concepts). The structure is furthermore adaptable because they must allow for the integration of new elements. Although we believe these network properties deemed for a qualitative difference with purely associative memory networks, arguably, some of them lacked a full empirical assessment in our experimental design. For example, while the notion that a semantic concept brings hierarchy into a memory network is well established in psychological models of memory representation (e.g., Collins and Quillian 1969), it would be important to determine the extent to which participants activate purely conceptual memory representation during learning in our experiment. Similarly, it would be important to determine the extent to which the decrease in generalization performance seen in the schematic/semantic condition, and the differences in EEG data, cannot be, at least partially, attributed to an increase of interference driven by the need to integrate more asso-

ciations in schematic/semantic than in simple memory networks from LP1. For instance, healthy controls in experiment 2, where the number of pair associations during encoding was lower than in experiment 1 (in order to ensure successful learning in TLE patients) showed higher generalization accuracy rates in schematic/semantic condition as compared to participants in experiment 1. Undoubtedly, the study of reaction time patterns in participants' responses during learning would have helped inform about this possibility (i.e., longer RTs to trials from schematic/semantic than from simple condition in LP2). However, to exclude that possible differences between conditions in the temporal evolution of specific neural responses recorded from scalp EEG recordings could be attributed to artefactual signals derived from motor preparation and response, participants were required to refrain from responding within the temporal window of interest (i.e., while encoded pictures were present in the screen during 3 s). Another limitation of our study is the gender imbalance in our sample (i.e., 85% of participants were women). Thus, though the gender disproportion arises because of a random recruitment procedure in the general population, we should be cautious about whether this may affect its representativeness.

We observed that the learning-eliciting theta oscillations during the integration of novel information into an existing memory network may reflect its underlying organizational properties. Specifically, we found that theta activity persisted longer and was more spread when new information was linked to schematic/semantic memory networks than when novel items had to be integrated into memory networks with a simple structure. Thus, these results are in line with previous literature emphasizing the putative role of theta oscillations as a neural mechanisms through which the hippocampus and prefrontal cortex are coordinated during inferential learning (Backus et al. 2016; Sans-Dublanc et al. 2017). However, an intriguing question is why schematic/semantic integration is translated into more persistent theta activity. One plausible, yet speculative, explanation relates to recent findings in humans that showed that the theta rhythm has been linked to coding spatial distance (Bush et al. 2017; Vass et al. 2016), as well as more abstract semantic and temporal distances (Solomon et al. 2019). We reason that our theta findings, therefore, could be related to the additional level of abstraction demands necessary to successfully integrate pairs of images in the schematic/semantic condition. In the item recognition literature, it is generally agreed that the presentation of an external stimulus initiates a processing cascade that starts with low-level perceptual features in early visual areas, and progresses to increasingly higher levels of semantic integration and abstraction along the inferior temporal cortex (Carlson et al. 2013; Cichy, Pantazis, and Oliva 2014; Clarke and Tyler 2015; Lehky and Tanaka 2016; Martin et al. 2018; Serre, Oliva, and Poggio 2007). Similarly, the notion that external input processing follows a hierarchical information processing stream has been a hallmark in major theories of human memory networks (e.g., Collins and Quillian 1969). More specifically, these models maintain that nodes in the memory network are represented in a hierarchical fashion, and that activation also spreads in a hierarchical fashion in the network, that is, from a node to an immediately lower node and then to a node still lower in the hierarchy. For instance, activation of plant would first spread to flower and then to rose. One of the major assumptions in this spreading activation model is that the amount of activation reaching a node depends on the representational distance from the source of activation, which received empirical support from studies investigating reaction time data in adult participants (Sharifian & Samani 1997). Our findings that theta persisted longer in time during the integration of events related to schematic/semantic memory networks than those related to simple networks may thus fit to the idea that theta oscillations may signal memory trajectories in the representational space.

Prior literature has emphasized how inferential learning relies on mechanisms of memory reactivation (e.g., Zeithamova et al., 2012). These studies revealed that prior event details are reinstated at the encoding of related experiences and that this supports participants' ability to infer relationships between distinct events that share content. The current study builds upon and significantly extends prior studies by showing that the representational nature and temporal dynamics of such reactivation during inferential encoding depend on the organizational structure of the related memory network. Indeed, our representational similarity analysis revealed high correlation between EEG patterns elicited by events encoded in LP2 and EEG patterns triggered by related events from the previous LP1 phase. However, while we found a similarity increase in a large cluster of time points, from ~500 to 2500 ms stimulus onset, between EEG-elicited patterns with new and related events within the simple network, neural similarity between new events and related events within the schematic/semantic network was higher than in the simple network condition for a brief window of time. This differential pattern of similarity results suggests that the reactivation nature of prior memory events during integrative encoding may adapt as a function of the structural properties of the related memory network. Accordingly, novel events that largely overlap in content with episodic content from a simple memory network would entail a detailed reactivation of the related event. We reasoned that such an adaptive property of the memory systems would be optimal in our daily life activity, as most of our experienced events ultimately share a relationship with stored memories. We conjecture that an efficient regulatory mechanism may exist to avoid the costs of inducing memory reactivation of specific memories during the ongoing encoding, while maximizing the benefits of maintaining a linked memory representation of an encoded event with previously stored memory representations. We speculate that this regulatory mechanism may be guided by the ability of a reminder/cue to navigate throughout the representational memory space and rapidly find associated events. If they are found, then these memory representations are reactivated and integrated in a common representational space (i.e., simple network in the current experiment). However, when a given cue does not match a specific representation for an event, then it moves to higher levels of representation, such as the conceptual level, thereby maximizing the ability to keep the current encoded event related to other memories that overlap at this representational level, as in the schematic/semantic network condition in the present experiment. Intriguingly, the pattern of similarity results that we obtained in the schematic/semantic condition fit recent EEG findings in humans revealing that information flow during encoding and retrieval may be reversed in order (Linde-Domingo et al. 2019). Thus, while visual encoding starts with low-level perceptual followed by high-level abstract processing, the mnemonic stream can prioritize the access to conceptual information. Our finding that the EEG patterns from early temporal windows elicited by novel events were similar to EEG patterns elicited at a late temporal window by the related event within a schematic/semantic memory network suggests that a similar retrieval-oriented prioritization to access conceptual information may be engaged in the schematic/semantic condition in our study.

Taken together, our findings shed light on the neural mechanisms that support the integration of novel information into existing memory networks. Our central finding is that both simple and schematic/semantic structures of memory networks aid integrative encoding of new information via the hippocampus, but that they engage different theta and neural reactivation patterns. Theta oscillatory activity was more persistent and widespread when the encoded event was to be integrated into a schematic/semantic memory network, lending support to the notion that theta oscillations play an important role in inferential learning. On the other hand, a stronger and temporally extended reactivation of prior event memories was found during the encoding of events that were integrated into simple memory networks, thereby suggesting the existence of regulatory mechanisms that promote the reactivation of related memory events when they belong to a simple structure in which multiple events are linked by direct association within a network. More broadly, the results emphasize the flexible nature of memory, whereby novel experiences and organizational properties of stored knowledge interact to enable structured representation of information in an ever-changing environment.

Acknowledgements

This work was supported by Ministerio de Ciencia, Innovación y Universidades, which is part of Agencia Estatal de Investigación (AEI), through the project PSI2016-80489-P (Co-funded by European Regional Development Fund. ERDF, a way to build Europe), to L.F. We thank CERCA Programme/Generalitat de Catalunya for institutional support.

Credit Author Statement

B.N., D.D. and L.F. designed the experiment. B.N., J.S.P., M.S. and M.F. acquired the data. B.N., D.D. and L.F. analyzed the data. B.N. and L.F. wrote the manuscript.

Data and code availability

Data and code are available from the authors upon reasonable request

References

Backus, Alexander R., et al., 2016. Hippocampal-prefrontal theta oscillations support memory integration. Curr. Biol. 26 (4), 450–457.

Bartlett, F.C., 1932. Remembering: A study in experimental and social psychology. Cambridge University Press.

Blair, R.Clifford, Karniski, Walt, 1993. An alternative method for significance testing of waveform difference potentials. Psychophysiology 30 (5), 518–524. http://doi.wiley.com/10.1111/j.1469-8986.1993.tb02075.x. December 8, 2019.

Bowman, Caitlin R., Zeithamova, Dagmar, 2018. Abstract memory representations in the ventromedial prefrontal cortex and hippocampus support concept generalization. J. Neurosci. 38 (10), 2605–2614.

Bush, Daniel, et al., 2017. Human Hippocampal Theta power indicates movement onset and distance travelled. PNAS 114 (46), 12297–12302.

Carlson, Thomas, Tovar, David A., Alink, Arjen, Kriegeskorte, Nikolaus, 2013. Representational dynamics of object vision: the first 1000 Ms. J. Vis. 13 (10).

Cichy, Radoslaw Martin, Pantazis, Dimitrios, Oliva, Aude, 2014. Resolving human object recognition in space and time. Nat. Neurosci. 17 (3), 455–462.

Clarke, Alex, Tyler, Lorraine K., 2015. Understanding What We See: How We Derive Meaning From Vision. Trends Cogn. Sci. 19 (11), 677–687.

Collins, Allan M., Ross Quillian, M., 1969. Retrieval time from semantic memory. J.f Verb. Learn. Verb. Behav. 8 (2), 240–247.

Craik, Fergus IM, Lockhart, Robert S, 1972. 11 Journal of verbal learning and verbal behaviour. Lev. Process.: Framew. Mem. Res. 1.

Dusek, Jeffery A., Eichenbaum, Howard, 1997. The Hippocampus and memory for orderly stimulus relations. PNAS 94 (13), 7109–7114.

Eichenbaum, Howard, 2017. Memory: organization and control. Annu. Rev. Psychol. 68 (1), 19–45.

Ghosh, Vanessa E., Gilboa, Asaf, 2014. What is a memory schema? a historical perspective on current neuroscience literature. Neuropsychologia 53 (1), 104–114. http://www.ncbi.nlm.nih.gov/pubmed/24280650. March 26, 2020.

Greene, Anthony J., Gross, William L., Elsinger, Catherine L., Rao, Stephen M., 2006. An FMRI analysis of the human hippocampus: inference, context, and task awareness. J. Cogn. Neurosci. 18 (7), 1156–1173.

Groppe, David M., Urbach, Thomas P., Kutas, Marta, 2011. Mass univariate analysis of event-related brain potentials/fields I: a critical tutorial review. Psychophysiology 48 (12), 1711–1725.

Heckers, Stephan, et al., 2004. Hippocampal activation during transitive inference in humans. Hippocampus 14 (2), 153–162.

Langner, Oliver, et al., 2010. Presentation and validation of the radboud faces database. Cogn. Emot. 24 (8), 1377–1388.

Lehky, Sidney R., Tanaka, Keiji, 2016. Neural representation for object recognition in inferotemporal cortex. Curr. Opin. Neurobiol. 37, 23–35. http://www.ncbi.nlm.nih.gov/pubmed/26771242. March 26, 2020.

Linde-Domingo, Juan, Treder, Matthias S., Kerrén, Casper, Wimber, Maria, 2019. Evidence That Neural Information Flow Is Reversed between Object Perception and Object Reconstruction from Memory. Nat. Commun. 10 (1), 179. http://www.nature.com/articles/s41467-018-08080-2. December 8, 2019.

Maris, Eric, Oostenveld, Robert, 2007. Nonparametric statistical testing of EEG- and MEG–Data. J. Neurosci. Methods 164 (1), 177–190.

Martin, Chris B., et al., 2018. Integrative and distinctive coding of visual and conceptual object features in the ventral visual stream. eLife 7. http://www.ncbi.nlm.nih.gov/pubmed/29393853. March 26, 2020.

McKenzie, Sam, et al., 2014. Hippocampal representation of related and opposing memories develop within distinct, hierarchically organized neural schemas. Neuron 83 (1), 202–215.

Minear, Meredith, Park, Denise C., 2004. A lifespan database of adult facial stimuli. Behav. Res. Methods. Instrum. Comput. 36 (4), 630–633.

Packard, Pau A., et al., 2017. Semantic congruence accelerates the onset of the neural signals of successful memory encoding. J. Neurosci. 37 (2), 291–301.

Pajkert, Anna, et al., 2017. Memory integration in humans with hippocampal lesions. Hippocampus 27 (12), 1230–1238.

Preston, Alison R., Shrager, Yael, Dudukovic, Nicole M., Gabrieli, John D.E., 2004. Hippocampal contribution to the novel use of relational information in declarative memory. Hippocampus 14 (2), 148–152.

Sans-Dublanc, A., Mas-Herrero, E., Marco-Pallarés, J., Fuentemilla, L., 2017. Distinct neurophysiological mechanisms support the online formation of individual and across-episode memory representations. Cereb. Cortex 27 (9), 4314–4325.

Schlichting, Margaret L., Preston, Alison R., 2015. Memory Integration: neural mechanisms and implications for behavior. Curr. Opin. Behav. Sci. 1, 1–8.

Schlichting, M, Preston, Alison R., 2016. Hippocampal-medial prefrontal circuit supports memory updating during learning and post-encoding rest. Neurobiol. Learn. Mem. 134 (Part A), 91–106. http://dx.doi.org/10.1016/j.nlm.2015.11.005.

Serre, Thomas, Oliva, Aude, Poggio, Tomaso, 2007. A feedforward architecture accounts for rapid categorization. PNAS USA 104 (15), 6424–6429. http://www.pnas.org/cgi/doi/10.1073/pnas.0700622104. March 26, 2020.

Sharifian, F., Samani, R., 1997. Hierarchical spreading of activation. In: Sharifian, F. (Ed.), Proc. of the Conference on Language, Cognition, and Interpretation. IAU Press, Isfahan, pp. 1–10.

Silva, Marta, Baldassano, Christopher, Fuentemilla, Lluís, 2019. Rapid memory reactivation at movie event boundaries promotes episodic encoding. J. Neurosci. : Off. J. Soc. Neurosci. 39 (43), 8538–8548.

Solomon, Ethan A., Lega, Bradley C., Sperling, Michael R., Kahana, Michael J., 2019. Hippocampal Theta codes for distances in semantic and temporal spaces. Proc. Natl. Acad. Sci. 116 (48), 24343–24352. http://www.pnas.org/lookup/doi/10.1073/pnas.1906729116. December 8, 2019.

Sols, Ignasi, Dubrow, Sarah, Davachi, LilaLluís Fuentemilla Correspondence, 2017. Event boundaries trigger rapid memory reinstatement of the prior events to promote their representation in long-term memory. Curr. Biol. 27, 3499–3504. https://doi.org/10.1016/j.cub.2017.09.057. December 8, 2019.

Tse, Dorothy, et al., 2011. Schema-dependent gene activation. Science 333 (August), 891–895.

Van Kesteren, Marlieke T.R., Fernández, Guillén, Norris, David G., Hermans, Erno J., 2010. Persistent schema-dependent hippocampal-neocortical connectivity during memory encoding and postencoding rest in humans. PNAS 107 (16), 7550–7555.

Van Kesteren, Marlieke T.R., Ruiter, Dirk J., Fernández, Guillén, Henson, Richard N., 2012. How schema and novelty augment memory formation. Trends Neurosci. 35 (4), 211–219.

Vass, Lindsay K., et al., 2016. Oscillations go the distance: low-frequency human hippocampal oscillations code spatial distance in the absence of sensory cues during teleportation. Neuron 89 (6), 1180–1186.

Xiao, Jianxiong, et al., 2010. SUN Database: large-scale scene recognition from abbey to zoo. In: Proceedings of the IEEE Computer Society Conference on Computer Vision and Pattern Recognition, pp. 3485–3492.

Zeithamova, Dagmar, Dominick, April L., Preston, Alison R., 2012. Hippocampal and ventral medial prefrontal activation during retrieval-mediated learning supports novel inference. Neuron 75 (1), 168–179.